ULTRA-COMPACT, LOW-NOISE, AMPLITUDE-SENSITIVE AND PHASE-SENSITIVE INTEGRATED THIN-FILM GIANT MAGNETOIMPEDANCE SENSORS

Bin Luo[1*], *Xianfeng Liang*[1], *Huaihao Chen*[1], *Cai Müller*[2], *Paul Raschdorf*[2], *Phillip Durdaut*[2], *Michael Höft*[2], *Jeffrey McCord*[2*] *and Nian X. Sun*[1*]
[1] Northeastern University, Boston, Massachusetts, USA
[2] Kiel University, Kiel, Schleswig-Holstein, Germany

ABSTRACT

Giant Magnetoimpedance (GMI) sensors are increasingly researched for their high magnetic field sensitivity, excellent spatial resolution, and low power consumption. This paper demonstrates self-biased, low-noise GMI sensors utilizing SiO2\Ti\(NiFe\Ti)$_4$\Cu\(NiFe\Ti)$_4$\Ti thin films on silicon substrates through photolithography and sputtering techniques. The 5000 µm × 50 µm amplitude-sensitive GMI sensors showed a remarkable performance, with a limit of detection (LoD) of 56.9 pT and noise levels at 810 pT· $Hz^{-1/2}$. Additionally, the phase-sensitive sensors achieved an impressive magnetic noise performance of ~100 pT/√Hz, which was obtained at a zero bias magnetic field at 15 Hz, utilizing an 800 MHz AC driving frequency and −2 dBm input power. Their compact size and complementary metal oxide semiconductor (CMOS)-compatible integration into Micro-Electro-Mechanical Systems (MEMS) underline their potential for advanced magnetic field sensing applications.

KEYWORDS

Giant Magnetoimpedance (GMI) Sensors, Magnetic Noise, Micro-Electro-Mechanical Systems (MEMS), Thin-Film Technology.

INTRODUCTION

Magnetic sensors are crucial in diverse engineering and industrial sectors, underpinning many modern technologies. Among the various types of magnetic sensors, Giant Magnetoimpedance (GMI) sensors have gained prominence due to their moderate to high magnetic field sensitivity, excellent spatial resolution, low production cost, and minimal power consumption [1-5]. The GMI effect—significant changes in AC impedance of a soft magnetic conductor under an external DC magnetic field—is primarily influenced by the skin effect and ferromagnetic resonance (FMR). Since its discovery in 1994 by Panina and Mohri [6, 7], researchers have refined GMI sensor technology, enhancing field sensitivity and reducing magnetic noise through innovative methods like LC-resonance circuits [8, 9], amplitude-modulation techniques [10], and linear differential-type sensors [11]. Recent advancements focus on using ribbons or microwires made from materials like CoFeSiB [12], which demonstrate potential for picotesla-level noise. However, traditional ribbon or microwire manufacturing techniques, such as glass-coated melt-spinning and electrodeposition [13, 14], are often costly and not suited for sensor integration, limiting broader application in modern technology.

Recognizing the potential of thin-film GMI sensors owing to their compact size, recent research has leveraged low-cost, complementary metal oxide semiconductor (CMOS)-compatible fabrication processes such as sputtering [15-20]. Multilayer structures, comprising non-magnetic conductive layers sandwiched between soft ferromagnetic layers, have demonstrated heightened sensitivity for quantitative determination of the concentration of magnetic nanoparticles in ferrogels [19]. In contrast to the intensive study and efforts in reducing electronic conditioning noise for microwire and ribbon GMI sensors [11, 21-25], the limit of detection (LoD) or intrinsic magnetic noise level of the thin-film GMI elements at high driving frequency was rarely explored, which are key parameters for characterizing magnetic sensor performance.

This paper presents a significant stride forward in thin film integrated GMI sensors, distinctly setting itself apart from conventional counterparts in micro-nano fabrication technique, novel sensing mechanism at GHz frequencies, superior limit of detection (LoD), and low magnetic noise. Unlike traditional bulky ribbon or microwire structures by melt-spinning and electrodeposition [13, 14], we leverage thin-film technology, employing a sputtering and photolithography patterning approach on a silicon (Si) wafer. Our thin-film GMI sensors, featuring a Ti(5*nm*)/(NiFe(25*nm*)/Ti(5*nm*))$_4$/Cu(400*nm*)/(NiFe(25*nm*)/Ti(5*nm*))$_4$/Ti(5*nm*) multilayer structure, represent a paradigm shift toward miniaturization, cost-effectiveness, and compatibility with complementary metal oxide semiconductor (CMOS) fabrication processes. In comparison to established multilayer GMI sensors at kHz and MHz levels based on domain wall motion [16, 18, 20], our sensors utilize a novel sensing mechanism based on ferromagnetic resonance and spin waves at GHz frequencies and exhibit superior performance metrics, including a remarkable LOD of 56.9 pT and an intrinsic magnetic noise level of 810 pT/√Hz for an amplitude-sensitive GMI sensor. In terms of noise characterization, our exploration extends beyond traditional electronic conditioning noise [23-25] and magnetic noise under amplitude modulation [19], as we delve into phase noise performance across varied AC driving frequencies, DC bias magnetic fields, and input power levels. The best performance is realized with a fascinating magnetic noise performance of ~100 pT/√Hz at 15 Hz, where the input power and driving AC frequency are −2 dBm and 800 MHz, respectively. The fabricated self-biased, low-noise phase-sensitive GMI sensors hold great promise for future magnetic sensing applications requiring superior magnetic sensing capability.

MICRO-NANO FABRICATION OF INTEGRATED GMI SENSOR

The schematic of our integrated GMI sensor composed of ground-signal-ground (GSG) electrodes and a sandwiched magnetic multilayer stripe is shown in Figure 1. The fabrication process starts

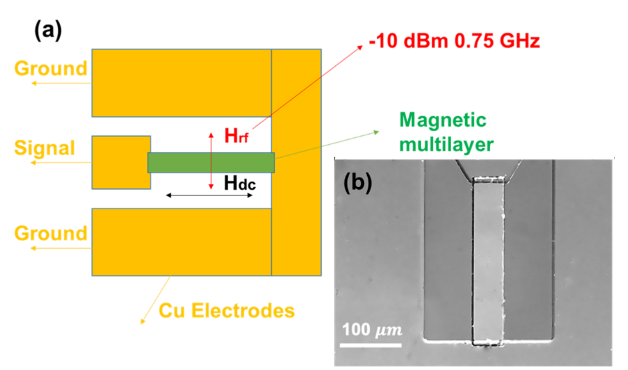

Figure 1: (a) Schematic of Ti/(NiFe/Ti)$_4$/Cu/(NiFe/Ti)$_4$/Ti thin film integrated GMI sensor. (b) Scanning electron microscopy (SEM) of magnetic multilayer strip.

978-1-940470-05-4/HH2024/$25©2024TRF
DOI 10.31438/TRF.HH2024.107

with a 3-inch Si (100) wafer with 500 nm insulating SiO_2 on top. A 200 nm thick gold film was evaporated and patterned by lift-off to form the GSG electrodes with good high-frequency electric performance. Then the wafer was diced into 14.5×9.5 mm^2 chips for magnetic film depositions and lift-off patterning. An in-situ magnetic field of 0.03 T was applied transversally to the longitudinal axis to induce a uniaxial in-plane magnetic anisotropy. The lengths and widths of multilayer strips were fabricated from 250 to 12500 µm and 20 to 200 µm, respectively.

AMPLITUDE-SENSITIVE GMI SENSOR

The maximum GMI ratio and sensitivity of a 1000 × 50 μm^2 element as a function of the magnetic fields and driving frequencies are obtained and presented in Figure 2 (a) and (b). The impedance changes and GMI ratio versus bias DC field along the long stripe edge were measured by probing S_{11} via a vector network analyzer. A large GMI ratio of 108.4% and sensitivity of 23.4 kΩ/T are realized at 0.8 GHz. We then measured detailed 2-D contour graphs of another batch 1000 × 50 μm^2 element as a function of the magnetic fields and AC driving frequencies, which are shown in Figure 2(c) and (d). The strongest GMI effect is caused by domain rotation in the intermediate frequency regime ranging from 0.1 to 1 GHz, where the maximum impedance peaks shift a little bit, and the maximum sensitivity peaks remain unchanged at ~700 µT. As the frequency goes up and higher than 1 GHz, the GMI sensors are in the FMR regime where the impedance peaks shift to higher fields with increasing frequency, The shift in peak position follows the Larmor condition and Kittel formula.

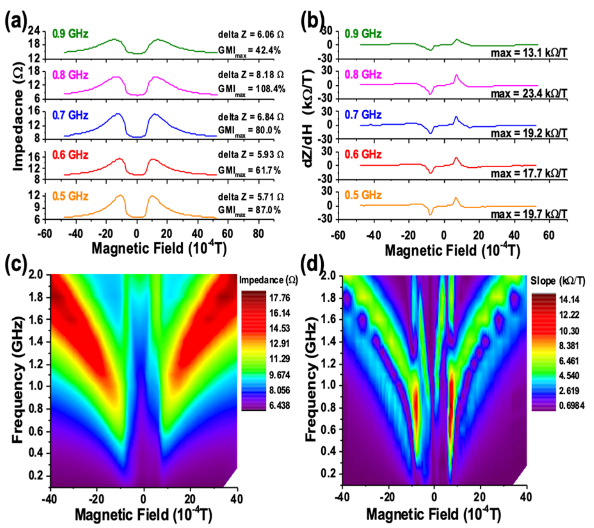

Figure 2. (a) Magnetoimpedance Z and (b) Impedance sensitivity dZ/dH as a function of magnetic fields and frequencies (0.5~0.9 GHz). Impedance change, GMI ratio and maximum dZ/dH are calculated. (c-d) 2-D colormap of Z and dZ/dH.

To investigate the LOD and magnetic noise performance of the fabricated thin-film GMI sensors, the power spectrum densities (PSD) were measured by an ultrahigh-frequency lock-in amplifier and a directional coupler when a 9.4 µT AC modulation field and 700 µT DC bias field were applied along the long stripe edge. The measurements were performed at several frequencies ranging from 1 to 1000 Hz. A low magnetic noise of 4.32 nT· $Hz^{-1/2}$ and LoD of 253 pT were demonstrated at 1 kHz, as shown in Figure 3. The notable enhancement of magnetic noise compared to LoD is due to the large electronic noise of the UHF lock-in system. We further fabricated a series of thin-film GMI sensors with the length of GMI element increased from 1000 µm to 12740 µm when the width is fixed to 50 µm. The best performance with a LoD of 56.9 pT and noise of 810 pT· $Hz^{-1/2}$ was acquired for the GMI sensor with a length of 5000 µm and width of 50 µm. With no need for complex electronic circuits, a large GMI ratio of 108.4% and low LoD of 56.9 pT were achieved, as shown in Figure 4. The low LoD, compact device size, as well as easy fabrication MEMS process, make these highly sensitive integrated radiofrequency (RF) GMI sensors promising candidates for future magnetic sensing applications.

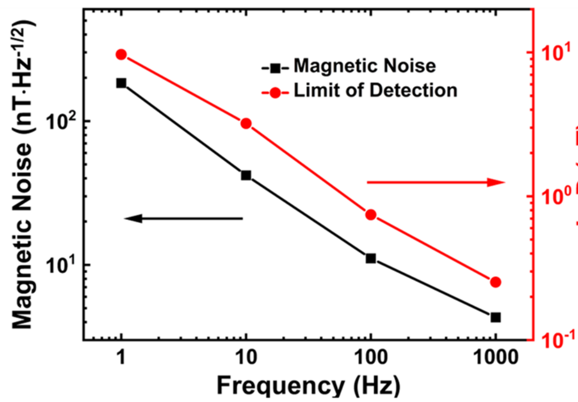

Figure 3. Magnetic noise and LoD as a function of frequencies for a 1000 µm ×50 µm GMI sensor, measured by UHF lock-in amplifier and a directional coupler.

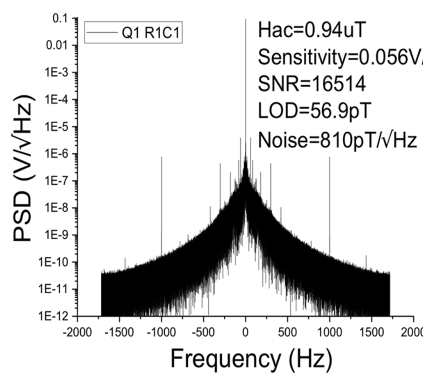

Figure 4: Power spectrum density (PSD) of a GMI sensor with optimized performance. The optimized sensor has a length of 5000 µm and a width of 50 µm.

PHASE SENSTIVE GMI SENSOR

We utilized the phase change of S_{21} of the GMI element to demonstrate phase sensitive GMI sensor for the first time. The GMI sensor exhibits a length of 12500 µm and 20 µm. The phase sensitivity, phase noise, and magnetic noise as a function of bias fields, AC driving frequencies, and input powers were investigated to explore the best operation point and evaluate the phase-sensitive GMI sensor performance. The GMI phase noise was measured by a phase noise analyzer.

As presented in Figure 5, we examined GMI phase-sensitive magnetic sensor performance as a function of bias fields. The magnetic field was swept from −5 mT to −1 mT. The AC driving frequency was fixed to 895.4 MHz where the phase sensitivity reaches a maximum of 15.91 rad/mT. The input power was maintained at −10 dBm. The phase sensitivity and phase noise rise when the magnetic field rises from −5 mT to −2.5 mT. The maximum phase sensitivity and phase noise were achieved at −2.5 mT, with maximum values of ~3×10^6 rad/T and ~5×10^{-2} rad^2/Hz,

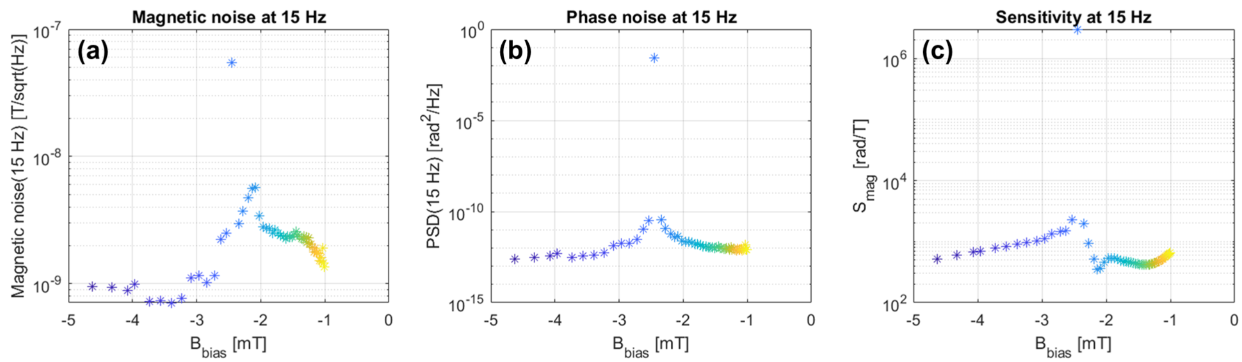

Figure 5: GMI phase magnetic sensor performance as a function of DC bias magnetic fields at the fixed frequency of 895.4 MHz and input power of −10 dBm at 15 Hz. (a) Magnetic noise defined as the square root of power spectrum density (PSD) divided by phase sensitivity.(b) Phase noise characterized by PSD. (c) Phase sensitivity.

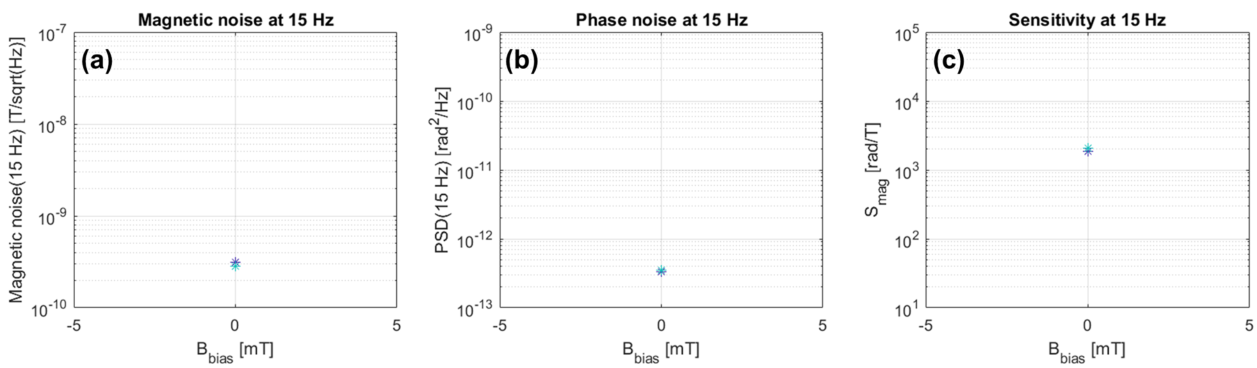

Figure 6: GMI phase magnetic sensor performance at zero DC bias magnetic fields at the fixed frequency of 895.4 MHz and input power of −10 dBm at 15 Hz. Cyan and blue stars represent forward (−5 mT to 0 mT) and backward direction (0 mT to −5 mT), respectively. (a) Magnetic noise defined as the square root of power spectrum density (PSD) divided by phase sensitivity.(b) Phase noise characterized by PSD. (c) Phase sensitivity.

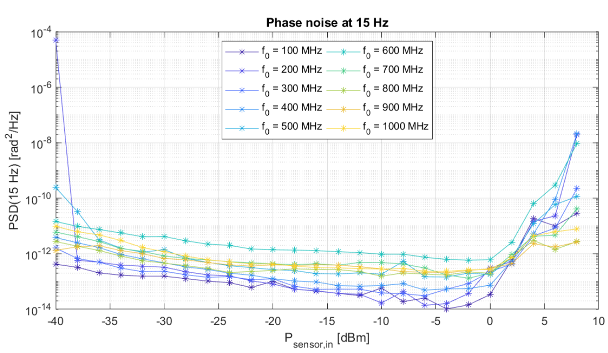

Figure 7. Phase noise characterized by phase power spectrum density (PSD) as a function of input power and AC driving frequency at the fixed zero bias field.

respectively. Despite the highest phase sensitivity near – 2.5 mT, the highest phase noise degrades the overall magnetic noise performance, leading to a high magnetic noise of ~5×10^{-8} T/√Hz. With the magnetic field increasing further from −2 mT to −1 mT, the phase sensitivity slightly fluctuates near 5×10^{2} rad/T, while the phase noise steadily decreases from ~2×10^{-12} rad^2/Hz to ~8×10^{-13} rad^2/Hz. Therefore, the overall magnetic noise decreases from ~3×10^{-9} T/√Hz to ~5×10^{-10} T/√Hz. We further examined GMI phase magnetic sensor performance at zero DC bias magnetic fields in forward (−5 mT to 0 mT) and backward directions (0 mT to −5 mT), as shown in Figure 6. At zero bias field, we achieved the best performance (fixed frequency 895.4 MHz, power −10 dBm) with a magnetic noise of ~300 pT/√Hz, which is quite different from other magnetic sensors typically operating on the points with maximum sensitivity, such as ME sensors [26].

As displayed in Figure 7, we measured the phase noise versus input power and driving frequency at zero bias field. The phase noise goes down linearly from −40 to −2 dBm and then goes up quickly. The best performance of the GMI phase magnetic sensor was realized at −2 dBm and 800 MHz, with the lowest magnetic noise reaching ~100 pT/√Hz. The lowest magnetic noise can be attributed to a high phase sensitivity and a substantially low phase noise. Giant GMI ratio and superior amplitude and phase magnetic noise performance position our integrated GMI sensor as a prospective amplitude-sensitive and phase-sensitive magnetic sensor, underscoring its multifaceted potential in advancing the landscape of magnetic sensing technologies.

CONCLUSION

In this study, a set of thin-film GMI sensors whose amplitude or phase is sensitive to magnetic fields have been developed using MEMS technology and subsequently characterized. Two straightforward experimental setups employing a UHF lock-in amplifier and a vector network analyzer were utilized to assess the GMI properties and the amplitude low detection of limit across a broad frequency spectrum. Remarkably, our amplitude GMI sensor achieved a high GMI ratio of 108.4% without the need for intricate electronic circuits. Through a detailed examination of the patterned Ti\(NiFe\Ti)$_4$\Cu\(NiFe\Ti)$_4$\Ti multilayer structure and its dimensions, the sensor demonstrated optimal performance, achieving an amplitude detection of limit of 56.9 pT and a noise level of 810 pT/√Hz. The combination of low limit of detection, compact size, and straightforward MEMS fabrication process positions these RF GMI sensors as highly promising for future applications in magnetic sensing. Additionally, the phase characteristics of phase-sensitive GMI sensors were explored using a phase analyzer, focusing on phase sensitivity, phase noise, and magnetic noise under various conditions of AC driving frequency, DC bias magnetic fields, and input power levels. The most effective performance was observed at zero bias magnetic field at 15 Hz, where the magnetic noise is improved to approximately 100 pT/√Hz. The sensors operated at a driving AC frequency of 800 MHz and an input power of −2 dBm. This newly developed low-noise, phase-sensitive GMI sensor is a promising step toward advanced self-biased integrated GMI sensors with enhanced capabilities for magnetic field detection.

ACKNOWLEDGEMENTS

Bin Luo, Xianfeng Liang, and Huaihao Chen contributed equally to this work and are co-first authors. This work is partially supported by the NIH Award UF1NS107694 and by the NSF TANMS ERC Award 1160504.

REFERENCES

[1] G. Kurlyandskaya, M. Sanchez and B. Hernando *et al.*, "Giant-magnetoimpedance-based sensitive element as a model for biosensors", *Applied Physics letters*, 82, 18 (2003).

[2] M. Phan, and H. Peng, "Giant magnetoimpedance materials: Fundamentals and applications", *Progress in Materials Science*, 53, 2 (2008).

[3] E. Fernández, G. Kurlyandskaya and A. García-Arribas *et al.*, "Nanostructured giant magneto-impedance multilayers deposited onto flexible substrates for low pressure sensing", *Nanoscale Research Letters*, 7 (2012).

[4] T. Uchiyama, K. Mohri and Y. Honkura *et al.*, "Recent Advances of Pico-Tesla Resolution Magneto-Impedance Sensor Based on Amorphous Wire CMOS IC MI Sensor", *IEEE Transactions on Magnetics*, 48, 11 (2012).

[5] D. Karnaushenko, D. D. Karnaushenko and D. Makarov *et al.*, "Self-Assembled On-Chip-Integrated Giant Magneto-Impedance Sensorics", *Advanced Materials*, 27, 42 (2015).

[6] L. Panina, K. Mohri and K. Bushida *et al.*, "Giant magneto-impedance and magneto-inductive effects in amorphous alloys," *Journal of Applied Physics*, 76, 10 (1994).

[7] L. Panina, K. Mohri and T. Uchiyama *et al.*, "Giant magneto-impedance in Co-rich amorphous wires and films.", *IEEE Transactions on Magnetics*, 31, 2 (1995).

[8] H. Lee, Y. S. Kim, and S. C. Yu, "Super-giant Magneto-Impedance Effect of a LC-resonator Using a Glass-Coated Amorphous Microwire", *Journal of Magnetics*, 7, 4 (2002).

[9] V. Raposo, M. Vázquez and A. Flores *et al.*, "Giant magnetoimpedance effect enhancement by circuit matching", *Sensors and Actuators a-Physical*, 106, 1-3 (2003).

[10] S. Yabukami, H. Mawatari and N. Horikoshi *et al.*, "A design of highly sensitive GMI sensor", *Journal of Magnetism and Magnetic Materials*, 290 (2005).

[11] G. Yu, X. Bu and B. Yang *et al.*, "Differential-Type GMI Magnetic Sensor Based on Longitudinal Excitation", *IEEE Sensors Journal*, 11, 10 (2011).

[12] P. S. Traore, A. Asfour, and J. P. Yonnet, "Design Approach for an Off-diagonal Giant Magneto Impedance Sensor Based on Field Programmable Gate Array", *Sensors & Transducers*, 245, 6 (2020).

[13] P. Squire, D. Atkinson and M. Gibbs *et al.*, "Amorphous wires and their applications", *Journal of Magnetism and Magnetic Materials*, 132, 1-3 (1994).

[14] X. Wang, W. Yuan and Z. Zhao *et al.*, "Giant magnetoimpedance effect in CuBe/NiFeB and CuBe/insulator/NiFeB electroless-deposited composite wires", *IEEE Transactions on Magnetics*, 41, 1 (2005).

[15] L. Panina, and K. Mohri, "Magneto-impedance in multilayer films", *Sensors and Actuators a-Physical*, 81, 1-3 (2000).

[16] E. Fernández, A. Lopez and A. Garcia-Arribas *et al.*, "High-Frequency Magnetoimpedance Response of Thin-Film Microstructures Using Coplanar Waveguides", *IEEE Transactions on Magnetics*, 51, 1 (2015).

[17] H. Kikuchi, S. Oe and H. Uetake *et al.*, "Enhancement of sensitivity on miniaturized thin-film magnetoimpedance with ellipsoidal element", *Physics Procedia*, 75 (2015).

[18] H. Kikuchi, S. Kamata and T. Nakai *et al.*, "Influence of demagnetizing field on thin-film GMI magnetic sensor elements with uniaxial magnetic anisotropy", *Sensors and Actuators a-Physical*, 230 (2015).

[19] G. Kurlyandskaya, E. Fernández and A. Safronov *et al.*, "Giant magnetoimpedance biosensor for ferrogel detection: Model system to evaluate properties of natural tissue", *Applied Physics Letters*, 106, 19 (2015).

[20] G. Buettel, J. Joppich, and U. Hartmann, "Micromachined silicon cantilevers with integrated high-frequency magnetoimpedance sensors for simultaneous strain and magnetic field detection", *Applied Physics Letters*, 111, 23(2017).

[21] S. Gudoshnikov, N. Usov and A. Nozdrin *et al.*, "Highly sensitive magnetometer based on the off-diagonal GMI effect in Co-rich glass-coated microwire", *Physica Status Solidi a-Applications and Materials Science*, 211, 5 (2014).

[22] L. Ding, S. Saez and C. Dolabdjian *et al.*, "Equivalent Magnetic Noise Limit of Low-Cost GMI Magnetometer", *IEEE Sensors Journal*, 9, 1-2(2009).

[23] B. Dufay, S. Saez and C. Dolabdjian *et al.*, "Improved GMI sensors using strongly-coupled thin pick-up coils", *Sensor Letters*, 7, 3 (2009).

[24] E. Fernández, A. García-Arribas and J. Barandiarán *et al.*, "Equivalent Magnetic Noise of Micro-Patterned Multilayer Thin Films Based GMI Microsensor", *IEEE Sensors Journal*, 15, 11 (2015).

[25] M. Malatek, B. Dufay and S. Saez *et al.*, "Improvement of the off-diagonal magnetoimpedance sensor white noise," *Sensors and Actuators a-Physical*, 204 (2013).

[26] T. Nan, Y. Hui and M. Rinaldi *et al.*, "Self-biased 215 MHz magnetoelectric NEMS resonator for ultra-sensitive DC magnetic field detection", *Scientific reports*, 3 (2013).

CONTACT

*Bin Luo, tel: +1-617-309-6845; luo.bin1@northeastern.edu
*Jeffrey McCord, tel: +49 431-880-6123; jmc@tf.uni-kiel.de
*Nian X. Sun, tel: +1-781-775-8878; n.sun@northeastern.edu